Slow-Wave Transmission Line Transformers/Baluns

BY

VAMSEE KRISHNA CHEKKA
B.Tech., Acharya Nagarjuna University, 2008

THESIS

Submitted as partial fulfillment of the requirements
for the degree of Master of Science in Electrical and Computer Engineering
in the Graduate College of the
University of Illinois at Chicago, 2012

Chicago, Illinois

Defense Committee:

H. Y. David Yang, Chair and Advisor
Danilo Erricolo
Piergiorgio L. E. Uslenghi

This Thesis is dedicated to my family and friends without whom it would never have been accomplished.

ACKNOWLEDGEMENTS

This project has been a very enlightening and rewarding experience for me in an area that is of great personal interest. I would like to acknowledge and express my gratitude to all those people who provided generous amounts of support and cooperation during this scholarly endeavor.

First of all I would like to express with immense pleasure my deep sense of gratitude to Professor H. Y. David Yang, my research advisor for his valuable suggestions and motivations in framing the research task, understanding the work and for guiding me with his fruitful remarks and advices throughout the project without whom this would have been impossible.

I would like to extend many thanks to student members of the Andrew Electromagnetics Laboratory for providing with the necessary software simulation resources and technical help through initial development and learning process till the successful completion. I also thank Prof. Danilo Erricolo and Prof. Uslenghi for willingness to be as thesis committee members.

I am very much thankful to my parents and friends for their extreme co-operation and motivating company throughout this endeavor.

VKC

TABLE OF CONTENTS

LIST OF FIGURES

LIST OF FIGURES (continued)

LIST OF ABBREVIATIONS

TLT	Transmission line transformer
SOC	System on chip
RFIC	Radio-frequency integrated circuit
VSWR	Voltage standing wave ratio
CRLH	Composite right/left handed
SWF	Slow-wave factor
MOM	Method of moment
RHTL	Right-handed transmission line
LHTL	Left-handed transmission line

SUMMARY

The miniaturization of RF passive components plays a vital role for SOC (system on-chip realization) fabrication and device size reduction on PCB's (printed-circuit board) design. RF component sizes are in proportion to the transmission-line wavelength. Conventional TLT (Transmission line transformer) or Baluns employing the use of magnetic cores become very lossy and inefficient beyond frequencies 10 MHz. Hence in recent times TLT's using the planar strip-lines with the distributed circuit approach that does not require the use of magnetic materials have been proposed.

In this thesis a novel technique is employed using the 3-D substrate metallization. Here the right-handed metamaterial guided wave structures are used which employs distributed series inductance and shunt capacitance achieved over multilayer loops and parallel strips of PCB. This will bring out the great increase in Slow-Wave Factor (SWR) which corresponds to component-size reduction. Lager SWF contributes to smaller guided wavelength, thereby the physical size of the RF passives can be reduced dramatically. A slow-wave TLT balun at 1.9GHz is characterized. A prototype is fabricated and tested. The full-wave simulation results from Zeland IE3D and network measurements find good agreement. The proposed TLT/baluns could be scaled up or down for applications in various wireless communication systems.

1. INTRODUCTION

1.1 Background and Motivation

RF passive components such as transformers/baluns realized on SOC's and on miniaturized PCB design substantially contribute to enhance the reliability, efficiency, and performance of RF integrated circuits. Extensive and innovative research has been done in recent times focusing on the design and characterization of various on-chip transformer models particularly achieving breakthroughs in device compactness and size reduction [1]. Transformers are typically used as impedance matching networks for antennas and amplifiers and as baluns for conversion between differential and single-ended signals. Wireless communication systems require baluns as one of the key components in devices such as balanced mixer, push-pull amplifier, and antenna feed networks etc. Analog circuits requiring balanced inputs and outputs in order to reduce noise and high order harmonics employ baluns.

As evident use of TLT's replacing the conventional transformers in device fabrication over past few decades is quite challenging. Transmission line transformers use novel design comprising interconnected transmission lines employing energy transfer through electromagnetic waves instead of the lossy coupling of flux method. These possess far wider bandwidths and much greater transmission efficiencies over the

conventional transformers. Use of the ferrite cores places limitations in the use of TLT's for higher frequencies because of the predominant core losses and parasitic effects. This limitation can be clipped by employing an alternate device fabrication technique removing the need for core. Thus use of planar transmission lines in TLT's aids in improving the transformer structures to facilitate more compactness, light weight and high packaging densities using the integrated circuit technology [2]. Use of multilayer technology has also greatly reduced the occupied space.

Hence modeling of TLT's using several planar strip fabrication techniques revolutionized SOC and PCB designs in recent years employing RF components. Several prototypes have been developed leading to more comprehensive and efficient performances.

One of the techniques employed for device miniaturization is by embedding them in high dielectric constant materials (smaller wavelengths) and this can be synthesized with 3-D material metallization built on a low dielectric medium on a multilayer PCB substrate [3-4]. Based on the recent research on Ultra – Slow wave transmission line structures (comprising distributed cascaded inductors and capacitors in a periodic manner) one could achieve high scales of size reduction involving novel high-density 3-D periodically loaded right-handed transmission lines. Here the SWF (defined as the ratio of free-space wavelength to the wavelength in the guided structure) is increased such that

smaller guided wavelengths are achieved and thereby reducing the physical size of the RF passives.

Based on the recent research related to developing a planar TLT from coreless high frequency switching power supply transformers aiming utilization in RF applications using multilayer technology the base topology of this thesis is constructed [5-8]. The topology consists of two quarter-wave transmission line structures cascaded and one of the line structures being made of interconnected lines to provide the DC isolation required [9]. The 3-D metallization technique bringing ultra-large slow-wave factor is applied to this topology resulting in a very compact Balun with length reduced to a factor less than one-tenth of the free-space wavelength.

A 1.9 GHz Balun is designed using a cascade of one 50 ohm and two 75 ohm ultra-slow wave transmission line structures connected and built over a 30-mil thick four layer FR-4 $(\varepsilon_r = 4.2)$ substrate where in the two 75 ohm lines are interconnected to provide the required DC isolation. The two quarter-wave lines are chosen in such a way that the characterized balun has a 1:9 impedance ratio at 1.9 GHz resulting in a 1:3 voltage ratio. The planar dimensions of this balun built on a 30mils thick FR-4 are 10mm by 6mm. A method of moment (MOM) based full-wave solver from Zeland called IE3D is used for simulations and various parameter extractions. This prototype is fabricated and tested.

The simulation results from IE3D and the measured results from network measurements find good agreement.

Thus the use of such innovative fabrication techniques for designing compact and physically miniaturized RF passives plays a significant role in the RF monolithic integrated circuits (RFIC's) design and device manufacturing at micro-electronic levels. These concepts can be improved further to be implemented to various other RF passives to achieve more efficient and high frequency operations.

2. THEORY

2.1 Theory for Transmission Line Transformer(TLT)/Balun

Transmission Line Transformer (TLT): Transmission line transformers operate by way transferring energy in the TEM mode of the transmission lines which is different from the way a regular conventional transformer energy transfer by means of magnetic flux coupling.

As discussed in the previous chapter Baluns are vital components in System on Chip (SOC) realizations and for PCB's layout in the RF Integrated Circuit Designs. The high frequencies operable baluns which are more compact, light weighted, energy efficient aid in various RFIC's applications such as balanced mixer, push-pull amplifier, and antenna feed networks etc. Analog circuits requiring balanced inputs and outputs in order to reduce noise and high order harmonics employ baluns. Thus the need for planar TLT's which unlike the conventional TLT's (i.e. operable only upto a range of less than 10MHz) that use core and hence placing limitations on the device compactness, fabrication and operation frequencies is quite evident. The design of planar TLT's and their characteristics are discussed in this chapter.First is described the analysis of general circuit parameters of a transmission line section and then DC Isolation is also achieved with the use of interconnected transmission lines.

2.2 **Analysis of a Transmission Line Section using Transmission (ABCD) Matrix**

In practice many microwave networks consists of a cascade connections two or many of two-port networks. Hence convenient way to characterize a microwave network would be to use 2×2 transmission or ABCD matrix for each two-port network. This derives that the final ABCD matrix for cascade of many two-port networks is nothing but the product of the ABCD matrices of the individual two-port networks in the same order as the connections are made.

Figure 1 shows a transmission line of length 'L'. Assuming this transmission line represents a two-port network one could get ABCD matrix to be defined as below

$$V_{in} = AV_L + BI_L \tag{2.1}$$

$$I_{in} = CV_L + DI_L \tag{2.2}$$

$$\begin{pmatrix} V_{in} \\ I_{in} \end{pmatrix} = \begin{pmatrix} A & B \\ C & D \end{pmatrix} \begin{pmatrix} V_L \\ I_L \end{pmatrix} \tag{2.3}$$

Where V_{in}, I_{in}, V_L and I_L are the input and output voltages and currents respectively and A, B, C and D are the elements of the ABCD matrix. The equations (2.1) and (2.2) show the basic relation between the input and output voltages and currents in this analysis [10-11].

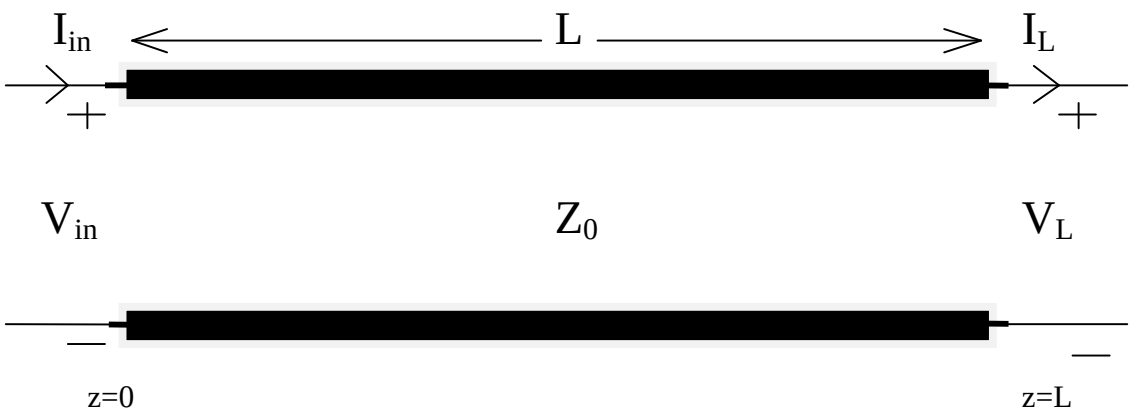

Figure 1 Transmission Line Section

'Z_0' is defined as the characteristic impedance of this transmission line section. From the transmission line equations the voltages and currents along the line can be given as

$$V(z) = V_1 e^{-\gamma z} + V_2 e^{\gamma z} \qquad (2.4)$$

$$I(z) = \frac{V_1 e^{-\gamma z} - V_2 e^{\gamma z}}{Z_0} \quad (2.5)$$

Where V(z) and I(z) are the voltages and currents along the line at any point 'z'. V_1,V_2 are the voltage amplitude constants. $\gamma = \alpha + j\beta$, where 'γ' is the propagation constant, 'α' is the attenuation constant and 'β' is the phase constant.

In order to obtain input and output voltages and currents we can substitute appropriate values for 'z' i.e. z= L for the output case and z=0 for the input case in the equations (2.4) and (2.5) respectively. Doing some simple algebraic manipulations using the four resulting equations one could determine the A, B, C and D elements of the ABCD matrix and the resulting equation is as follows

$$\begin{bmatrix} A & B \\ C & D \end{bmatrix} = \begin{bmatrix} \cosh(\gamma l) & Z_0 \sinh(\gamma l) \\ \frac{\sinh(\gamma l)}{Z_0} & \cosh(\gamma l) \end{bmatrix} \quad (2.6)$$

In case of a loseless transmission line we assume attenuation constant 'α' is 0. Hence the final ABCD matrix is

$$\begin{bmatrix} A & B \\ C & D \end{bmatrix} = \begin{bmatrix} \cos(\beta l) & jZ_0 \sin(\beta l) \\ j\frac{\sin(\beta l)}{Z_0} & \cos(\beta l) \end{bmatrix} \quad (2.7)$$

From equation (2.7) one could find the ratio of input and output impedance as follows,

$$\frac{\text{Zin}}{\text{ZL}} = \frac{\cos(\beta l) + j\sin(\beta l)\frac{(Z_0)}{Z_L}}{j\sin(\beta l)\frac{(Z_0)}{Z_L} + \cos(\beta l)} \tag{2.8}$$

If we assume the line is of quarter wavelength to obtain a linear and a non-complex relation between the input and output impedances, then for a quarter-wave transformer where in the 'L' is equal to ¼ of the wavelength 'λ'.

$$Z_{in} = \frac{{Z_0}^2}{Z_L} \tag{2.9}$$

The two important disadvantages that prohibits this single section of quarter-wavelength transmission line from being used as a transformer are

(i) First the transmission line is not DC isolated i.e. there is a common conductor path between the in put and output ports. A Balun/TLT when used at the output stage of the power supply the concept of DC isolation is very important because in most cases the load and power supply are grounded and this might result in short circuiting of the output components in the circuit.

(ii) Input and output impedances from the equation (2.9) can be related in a product form. That is a constant characteristic impedance for a given quarter-wave transmission line can be given by the geometric mean of the Z_{in} and Z_L values. Where as in the case of a convention transformer the input (primary) and the output (secondary) voltages and currents cannot be related in the same way to form a relation like that of (2.9) between their input/output impedances. In the conventional transformer the impedance ration between primary and secondary ports is of the form

$$\frac{Z_{in}}{Z_L} = \frac{1}{N^2} \qquad (2.10)$$

Where $Z_{in}= V_{in}/I_{in}$, $Z_L= V_L/I_L$ are the impedances at the primary and the secondary ends. 'N' is the reciprocal of the voltage ratio and the current ratio between the input (primary) and the output (secondary) ports.

2.3 Electrical Isolation of Two Two-Wire Transmission Lines

To clip the cited disadvantages and to use a quarter-wavelength transformer as a conventional transformer the following methods have been adopted. It is known that two two-wire transmission lines can be interconnected in a manner that the input and

output ports are electrically isolated. The resulting isolated interconnected lines are shown in Figure 2 as in [12].

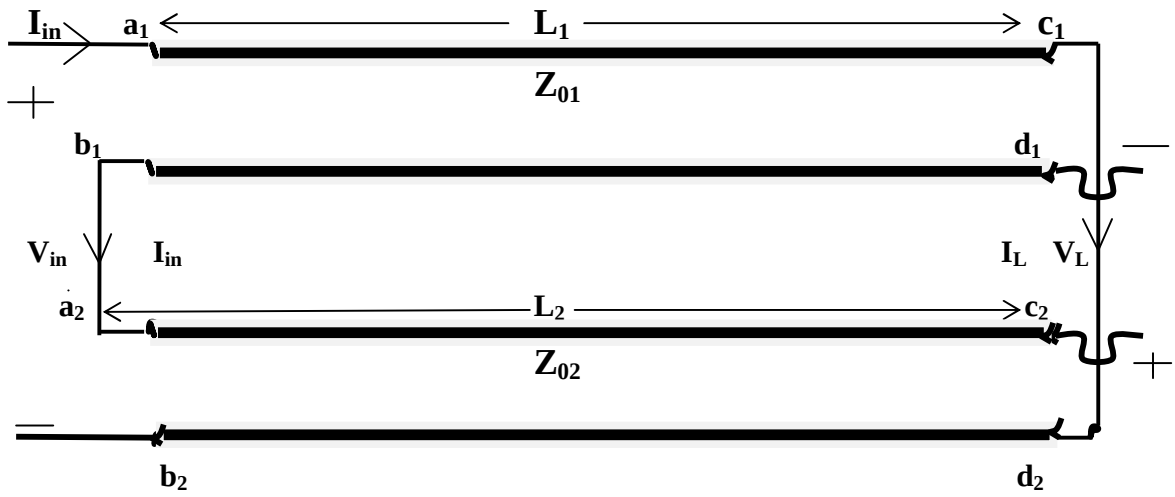

Figure 2 Isolated Interconnected Transmission Lines

In order to obtain the circuit parameters for the interconnected transmission lines and to derive the combined ABCD transmission matrix one should make the balanced line transmission line assumption. With that assumption the current in one conductor of the transmission line is equal in magnitude and opposite in direction to the other. This makes the current I_{in} going into the node a_2 same as the current emerging from the node b_1.

Same is the case with current I_L that is going into node d_2 to be same as the current emerging from node c_1. Assuming Z_{01} and Z_{02} are the characteristic impedances, L_1 and L_2 being respective lengths of the each of the individual transmission lines, one can obtain a final ABCD matrix for equal electrical lengths, i.e.

$$\beta_1 L_1=\beta_2 L_2=\beta L$$

$$\begin{bmatrix} A & B \\ C & D \end{bmatrix} = \begin{bmatrix} \cos(\beta l) & j\sin(\beta l)(Z_{01}+Z_{02}) \\ j\dfrac{\sin(\beta l)}{(Z_{01}+Z_{02})} & \cos(\beta l) \end{bmatrix} \tag{2.11}$$

Where 'β_1' and 'β_2' are phase constants of 1 and 2 transmission lines respectively.

From equation (2.11) one can infer that the final matrix ABCD of the interconnected transmission lines from Figure 2 is very similar to that of a single section matrix. To further simplify if we further assume,

$$Z_0=Z_{01}+Z_{02}$$

Then an interesting assumption can be made. One can state that the transmission matrix resulting from the interconnection of two transmission lines of equal physical length, equal phase constants is similar to a single transmission line section which has the same phase constant, length but the characteristic impedance is the sum of the

characteristic impedances of each of the individual lines and can represented in by the Figure 3 as follows

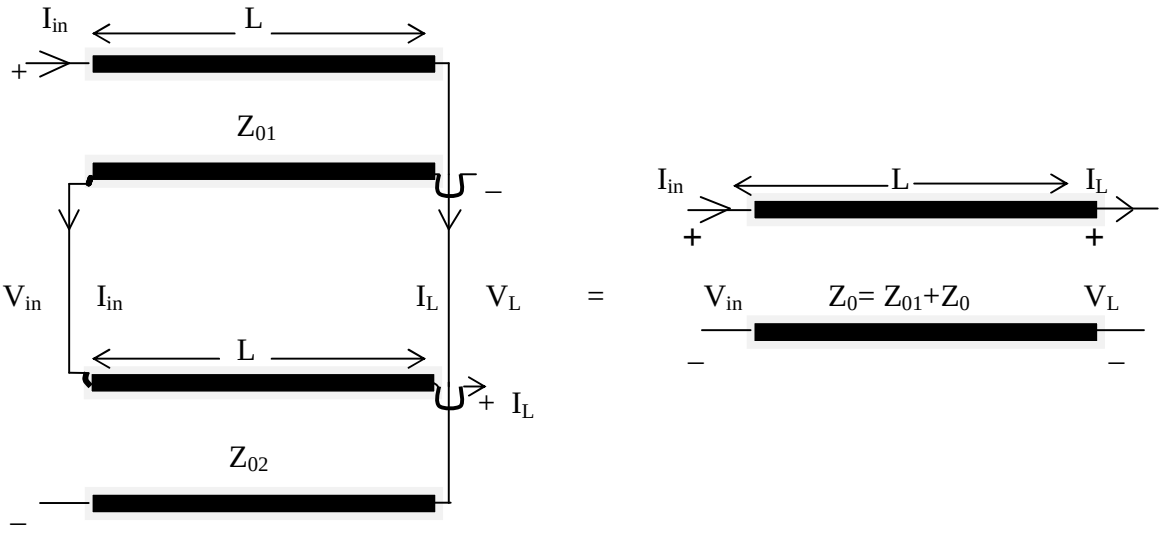

Figure 3 Equivalent Transmission Lines

Hence the desired electrical isolation is obtained. A useful feature of the interconnected lines is that the input and output signals are dc isolated similar to a power transformer. Furthermore, the symmetry allows the output to be differential for a balun operation.

2.4 **Conventional Transformer Response**

From section 2.2 which contains a simple single quarter-wave transmission line one could not obtain the required response as that of a conventional transformer and same is the case even when dealt with the electrically isolated interconnected transmission lines. In order to overcome this dis-advantage one could use two such isolated and interconnected two line quarter-wave transformer sections and cascade them to get response of a conventional transformer. It is known that two quarter-wave transformers cascaded together form an impedance transformer, where the voltage ratio is the ratio of the characteristic impedance of the two lines. First using the equation (2.11) one should obtain the ABCD matrix for each of the individual cascaded sections and the final matrix for the entire transformer can be obtained by the product of these matrices. The following Figure 4 shows one such cascaded transmission line transformer as,

Figure 4 Transmission Line Transformer with two quarter-wave transformers cascaded together forming an impedance transformer

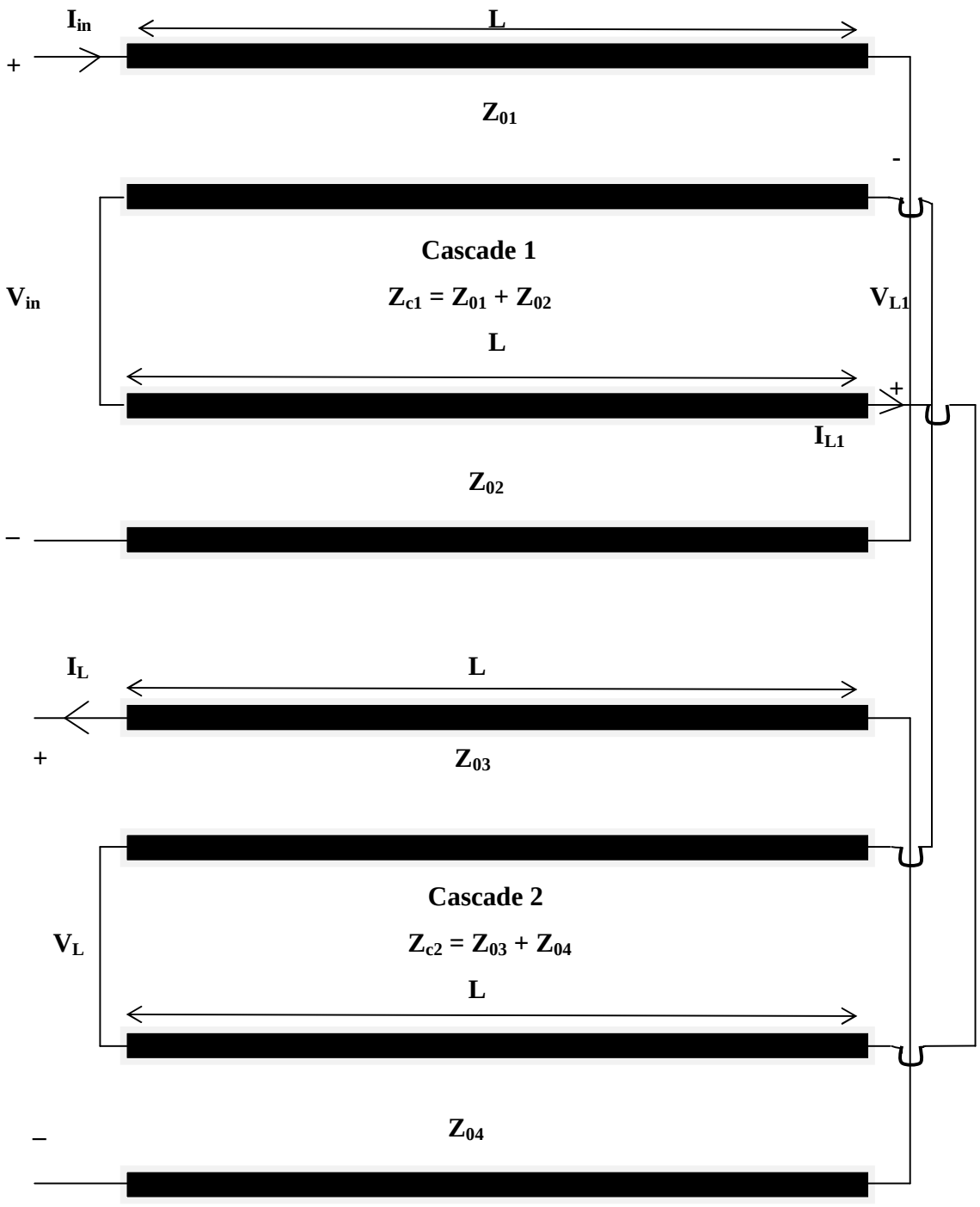
I_{in}
L
+
Z_{01}
-
Cascade 1
$Z_{c1} = Z_{01} + Z_{02}$
V_{in}
V_{L1}
L
+
I_{L1}
Z_{02}
–
I_L
L
+
Z_{03}
Cascade 2
$Z_{c2} = Z_{03} + Z_{04}$
V_L
L
–
Z_{04}

The transmission matrix for the cascade section one is,

$$\begin{pmatrix} V_{in} \\ I_{in} \end{pmatrix} = \begin{pmatrix} A_1 & B_1 \\ C_1 & D_1 \end{pmatrix} \begin{pmatrix} V_{L1} \\ I_{L1} \end{pmatrix} \qquad (2.12)$$

for the cascade section two,

$$\begin{pmatrix} V_{L1} \\ I_{L1} \end{pmatrix} = \begin{pmatrix} A_2 & B_2 \\ C_2 & D_2 \end{pmatrix} \begin{pmatrix} V_L \\ I_L \end{pmatrix} \qquad (2.13)$$

and for the entire transformer,

$$\begin{pmatrix} V_{in} \\ I_{in} \end{pmatrix} = \begin{pmatrix} A & B \\ C & D \end{pmatrix} \begin{pmatrix} V_L \\ I_L \end{pmatrix} \qquad (2.14)$$

From equations (2.12) and (2.13), one could observe the final matrix ABCD for the TLT is same as the product of the individual cascaded sections $A_1B_1C_1D_1$ and $A_2B_2C_2D_2$. Hence we have,

$$\begin{bmatrix} A & B \\ C & D \end{bmatrix} = \begin{bmatrix} A1A2 + B1C2 & A1B2 + B1D2 \\ C1A2 + C2D1 & B2C1 + D1D2 \end{bmatrix} \qquad (2.15)$$

From equation (2.11) one could write the transmission matrices related to their individual cascaded sections as,

$$\begin{bmatrix} A_1 & B_1 \\ C_1 & D_1 \end{bmatrix} = \begin{bmatrix} \cos(\beta l) & j\sin(\beta l)(Z_{c1}) \\ j\,\frac{\sin(\beta l)}{(Z_{c1})} & \cos(\beta l) \end{bmatrix} \qquad (2.16)$$

$$\begin{bmatrix} A_2 & B_2 \\ C_2 & D_2 \end{bmatrix} = \begin{bmatrix} \cos(\beta l) & j\sin(\beta l)(Z_{c2}) \\ j\,\frac{\sin(\beta l)}{(Z_{c2})} & \cos(\beta l) \end{bmatrix} \qquad (2.17)$$

Hence from equation (2.15), one could get

$$\begin{bmatrix} A & B \\ C & D \end{bmatrix} = \begin{bmatrix} \cos^2(\beta l) - \sin^2(\beta l)\frac{Z_{c1}}{Z_{c2}} & j\sin(\beta l)\cos(\beta l)(Z_{c1} + Z_{c2}) \\ j\sin(\beta l)\cos(\beta l)(\frac{1}{Z_{c1}} + \frac{1}{Z_{c2}}) & \cos^2(\beta l) - \sin^2(\beta l)\frac{Z_{c2}}{Z_{c1}} \end{bmatrix} \qquad (2.18)$$

Where $Z_{c1}= Z_{01}+Z_{02}$, $Z_{c2} = Z_{03}+Z_{04}$ are characteristic impedances of the individual cascade sections one and two respectively, since from previous sections one could assume such interconnected isolated transmission lines as a single section of line with characteristic impedance equal to their sum.

If we define the normalized characteristic impedances for cascaded sections one and two as,

$$Z_{c1}=Z_{C1}/Z_L,$$

$$Z_{c2}=Z_{C2}/Z_L,$$

and the impedance ratio for the entire cascaded section as,

$$N= Z_{c2}/ Z_{c1},$$

From the transmission matrix equations,

$$V_{in}= AV_L+ BI_L$$

$$I_{in} = CV_L+DI_L$$

One could obtain the ratios V_{in}/V_L and I_{in} /I_l values as $A+B/(Z_l)$ and CZ_l+D,

Having known the values for A,B,C,D values from equation (2.18) we can substitute these values and obtain the voltage, current and impedance ratio characteristics for the TLT as,

$$\frac{Z_{in}}{Z_L} = \frac{\frac{V_{in}}{V_L}}{\frac{I_{in}}{I_L}}$$

$$= \frac{\cos^2(\beta l) - \frac{\sin^2(\beta l)}{N} + j\sin^2(\beta l)\frac{(Z_{c1} + Z_{c2})}{\tan(\beta l)}}{\cos^2(\beta l) - \sin^2(\beta l)N + j\sin^2(\beta l)\frac{(\frac{1}{Z_{c1}} + \frac{1}{Z_{c2}})}{\tan(\beta l)}}$$

(2.19)

at quarter wavelength equation (2.19) reduces to,

$$\frac{Z_{in}}{Z_L} = \frac{\frac{V_{in}}{V_L}}{\frac{I_{in}}{I_L}} = \frac{\frac{1}{N}}{N} = \frac{1}{N^2}$$

(2.20)

This gives the voltage/current/impedance characteristics similar to that of a conventional transformer, where in the ratio of the input to output impedance is inverse of the square of real number and that implies the voltage/current ratio is inverse of that number and can be matched with the equation from (2.10) for a conventional transformer.

The Transmission line transformer circuit topology shown in the Figure 4 can be further simplified by recollecting that the isolated interconnected quarter-wave transmission lines can be equivalent to that of a single section with impedance equal to the combination of the individual line sections and also represented in Figure 3. Hence in Figure 4 if the cascade section one is replaced by a single section of line with equivalent

characteristic impedance then their will be no effect on over-all performance of the circuit and the total number transmission lines used in the circuit topology is now reduced from four to three thus reducing the total physical length of the transformer by 25%. This modified structure of the TLT can be seen from the Figure 5.

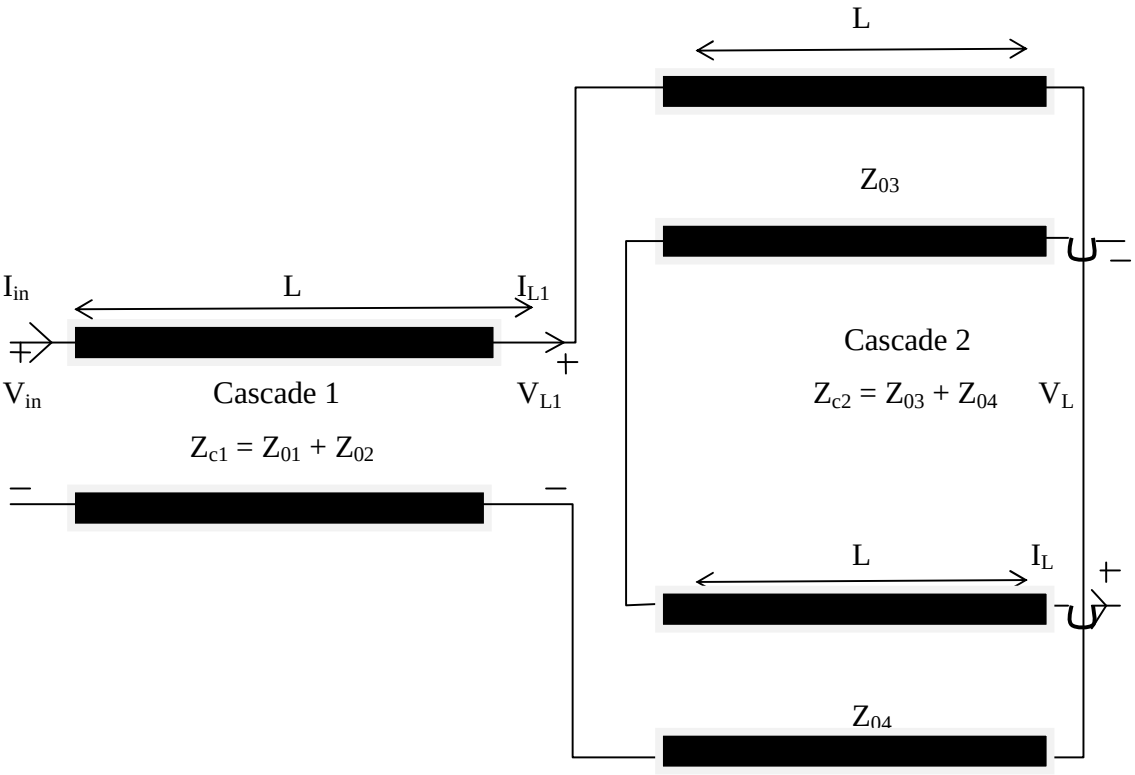

Figure 5 Transmission Line Transformer (TLT) with three transmission Lines

Hence the required topology for transmission line transformer (TLT) is designed using three transmission line sections, which is having identical response with that of a conventional transformer and also provided with electrical isolation and hence can be used as an effective Balun. In contrast to a Marchand balun where the input port is DC open with 50ohm output termination, the TLT balun input port carrying the basic features of a power transformer is dc short and serves as impedance as well as voltage transformer. In RF applications, it could connect to high-impedance differential amplifiers at chip levels.

2.5 **Characteristics of Metamaterial Slow-wave Periodic Structures:**

Metamaterials are artificially structured materials physically modified to have properties that may naturally are not existent in them. Metamaterials usually gain their properties from structure rather than composition, using small irregularities to embed significant changes in their efficiencies. The study of the fundamental electromagnetic properties of the slow-wave periodic structures using general transmission line approach provides insight for designing novel miniaturized microwave devices.

Periodic structures have been significantly developed in the recent past in various applications of microwave engineering. In nature crystal structures exist with well defined periodicity. Periodic structures are nothing but finite or infinite repetition of a unit cell in one, two or three dimensions. Metamaterial periodic structures have been the centre of research for efficient use in device compactness, fabrication density and weight reduction techniques development. Metamaterials are considered highly efficient when compared with the traditional di-electric materials and conducting metals. Metamaterials have found profound use in many practical applications in microwave and optical fields. Some of the typical examples include microwave filters, couplers, lenses, beam steerers, modulators etc. Photonic crystals and frequency selective surfaces are some other periodic structures that can be talked about while the distinct feature of metamaterials is that these are pre-defined for specific applications irrespective of the former.

Arrays of distributed current conducting elements like inductors and capacitors characterized by multilayer wounded wire loops and parallel strips contribute to microwave frequency metamaterials. Electromagnetic band-gap and dispersion curves can also be tailored in the usage of these structures. The conventional transmission lines (TL's) consists of series inductance and shunt capacitance in the circuit model of their unit cells.

Conventional TL's are a typical example of a right-handed RH materials where in the electromagnetic energy as well as the wave-fronts travel away from the source and also the phase and group velocities are parallel with each other. The typical example to increase a slow-wave factor is to significantly raise the inductive and capacitive values in the distributed structures. The SWF (slow-wave factor) is defined as the ratio of the free-space wavelength to guided wavelength. By using these SWF increasing techniques one could enormously reduce the device size and thus increase the operating frequencies i.e. bandwidth. The other structures that are mirror image to RH TL's are nothing but the left-handed (LH) TL's. These have circuit models for unit cells where in the inductance and capacitance are interchanged which results in opposite phase and group velocities unlike the RH materials in which the phase and group velocities are parallel. The main focus of our study is on the RH periodic structures that provide better and stable SWF and least dispersive characteristics when compared with LH materials over the broad frequency ranges.

Next we study the transmission line analysis of the infinite periodic structures and then characteristics of the slow-wave RH structures are analyzed.

2.6 **Transmission Line Analysis of Infinite Periodic Structures**

Let us consider an infinite periodically loaded transmission line as below,

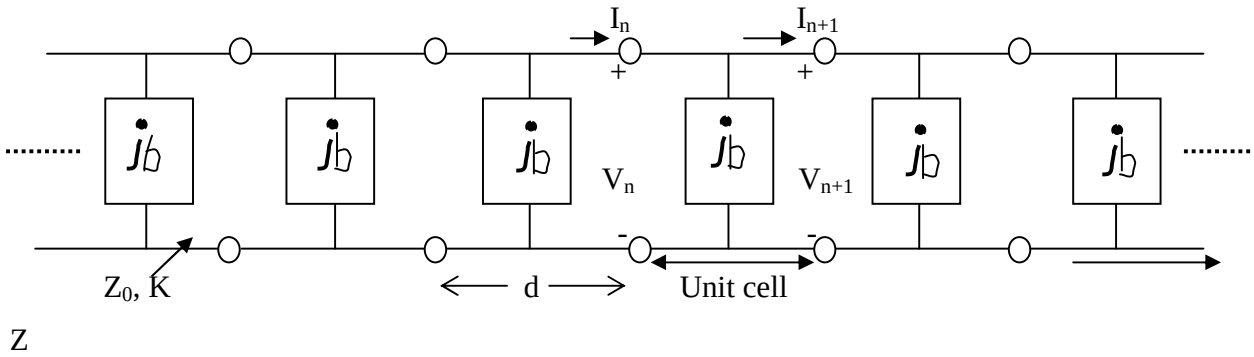

Z

Figure 6 Infinite periodically loaded transmission line

Here the unit cell for the infinite transmission line consists of the length ‘d’ of the transmission line in which we can find shunt susceptance of the value ‘b’. The value ‘b’ is normalized to the value of the characteristic impedance Z_o. If the infinite line is considered to have an infinite number of two-port networks than a transmission matrix written for the n_{th} cell is given with A,B,C, and D parameters that related the voltages and currents on either of the cell as in [13],

$$\begin{pmatrix} V_n \\ I_n \end{pmatrix} = \begin{pmatrix} A & B \\ C & D \end{pmatrix} \begin{pmatrix} V_{n+1} \\ I_{n+1} \end{pmatrix} \tag{2.21}$$

The unit transmission line section consists of a line of length d/2, and then the susceptance 'b' and then again the line of length d/2. The combined matrix for this cascaded section is written as

$$\begin{bmatrix} A & B \\ C & D \end{bmatrix} = \begin{bmatrix} (\cos\theta - \frac{b}{2}\sin\theta) & j(\sin\theta + \frac{b}{2}\cos\theta - \frac{b}{2}) \\ j(\sin\theta + \frac{b}{2}\cos\theta + \frac{b}{2}) & (\cos\theta - \frac{b}{2}\sin\theta) \end{bmatrix} \tag{2.22}$$

Assuming the wave is propagating in the +Z direction and since the line is infinitely long, the voltage and current at the n_{th} terminal can only differ by a phase delay factor of $e^{-\gamma d}$, where 'ɤ' is the complex propagation constant and ɤ=α+jβ. Thus,

$$V_{n+1} = V_n e^{-\gamma d}$$

$$I_{n+1} = I_n e^{-\gamma d} \tag{2.23}$$

Combining equations (2.21) and (2.23) we have

$$\begin{pmatrix} A - e^{\gamma d} & B \\ C & D - e^{\gamma d} \end{pmatrix} \begin{pmatrix} V_{n+1} \\ I_{n+1} \end{pmatrix} = 0 \tag{2.24}$$

In order to determine the non-trivial solution for the above matrix the determinant should be '0'. This results in the following eigen-value equation after performing some simple algebraic manipulations [13],

$$\cosh \gamma d = \frac{A+D}{2} \qquad (2.25)$$

The characteristic impedance of these waves at the unit cell terminals is defined as

$$Z_B = Z_0 \frac{V_{n+1}}{I_{n+1}} \qquad (2.26)$$

'Z_o' is the characteristic impedance of the unloaded line. Since these waves are similar to the elastic waves or Bloch Waves that travel through periodic crystal lattices, the impedance Z_B is also referred to as Bloch impedance. From equations (2.24) and (2.26) we can solve for Z_B as in [13],

$$Z_B \pm = \frac{-2BZ_0}{2A-A-D \mp \sqrt{(A+D)^2-4}} \qquad (2.27)$$

The $\pm$ sign indicates the characteristic impedance for positively and negatively travelling waves. Here the direction in which I_n travels is referred to as the positive direction. If the magnitude of the ($\cosh \gamma d$) value is ≤ 1 and Z_B is purely real, the periodic structure support the propagating modes; if magnitude of ($\cosh \gamma d$) is > 1 and Z_B is purely imaginary, which results in a rapid exponential delay of the fields in the cut-off modes.

Now let us consider the analysis of a unit cell which consists a lumped LC network on the transmission line with length ‘d’ being much smaller than the wavelength of interest. The lossless TL is assumed throughout the analysis.

2.7 **Analysis of Transmission line loaded with reactive elements**

In this analysis the lossless transmission line consists of cascades of reactive elements like L and C as shown in Figure 7. Thus the line is formed by the cascades of LC networks. When considering the transmission line to be acting as a filter, this LC based TL is a low-pass filter. Care is taken that the unit length of the cell ‘d’ is smaller than the guided wavelength i.e. say $d < \lambda_g / 4$ i.e. the electrical length of the unit cell is smaller than the $\pi / 2$, then the LC based TL is primarily considered as the homogenous medium by electromagnetic waves. This is purely right-handed because the wave propagation follows right-hand rule. By simply replacing the inductance by capacitance and vice versa one could achieve the high-pass filter action of the TL and the resulting structure is left-handed LH. The main focus in this thesis is only on the RH structures because of the low dispersion effects being considered into account over a wide range of frequencies.

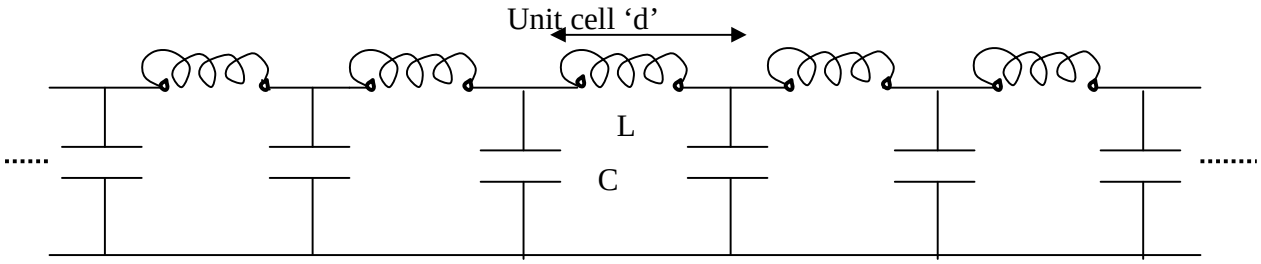

Figure 7 Lumped- element low-pass LC network

2.7.1 **Propagation characteristics of a Slow- Wave structure**

For the unit cell circuit shown in the fig 2.7 the transmission matrix ABCD is given by, For an inductor L and circular frequency ‘ω’ the ABCD matrix is

$$\begin{bmatrix} 1 & j\omega L \\ 0 & 1 \end{bmatrix}$$

Similarly for capacitor with capacitance C the ABCD matrix is

$$\begin{bmatrix} 1 & 0 \\ j\omega C & 1 \end{bmatrix}$$

Hence for the unit cell the matrix is,

$$\begin{bmatrix} A & B \\ C & D \end{bmatrix} = \begin{bmatrix} 1 & j\omega L \\ 0 & 1 \end{bmatrix} \begin{bmatrix} 1 & 0 \\ j\omega C & 1 \end{bmatrix} = \begin{bmatrix} 1 - \omega^2 LC & j\omega L \\ j\omega L & 1 \end{bmatrix}$$

(2.27)

Based on the equation from (2.25), and also considering $\gamma=\beta$, since $\alpha=0$ for the lossless case we have,

$$\cos \beta d = 1 - \frac{\omega^2 LC}{2} \qquad (2.28)$$

The eigen value 'β' can be solved assuming that the right hand side of the equation (2.28) is not more than 1 because cosine values are defined only for values between 0 and 1. Hence the cut-off frequency can be defined for the proposed structure above and hence the structure behaves as a low-pass filter and the stop band for the structure appears. If the maximum value i.e. '1' is considered for '$1 - \frac{\omega^2 LC}{2}$,' then we have,

$$f_c = \frac{1}{\pi\sqrt{LC}} \qquad (2.29)$$

Then the phase constant β can be derived in terms of cut-off frequency f_c as

$$\beta = \frac{1}{d} . \cos^{-1}\left[1 - 2\left(\frac{f}{f_c}\right)^2\right] \qquad (2.30)$$

The most important parameter, slow-wave factor (SWF) is defined as the ratio of the phase constant β normalized to the free-space constant k_o ,

$$SWF = \frac{\beta}{k_0} = \frac{\lambda_0}{\lambda_g} \qquad (2.31)$$

Where $k_0 = C_0/f$ and $C_0 = 3*10^8$ m/s is the speed of light in free space, λ_o is the wave length in free space and λ_g is the wavelength of the periodic structure.

From the equation for the SWF one can observe that the SWF is inversely proportional to the guided wavelength which implies that the increase in value of the SWF will significantly result in reduction of the guided wavelength. The physical sizes of RF passives are normally dependent on the guided wavelength and are comparable with their electrical lengths and hence the reduction in the size is achieved. Similar kind of results can be obtained when a component is embedded in a high di-electric constant material. Hence metamaterials with large SWF results in component size reduction. The phase velocity of the propagating mode decreases since the SWF increases and hence the name “Slow-Wave mode” for the propagation.

The lumped element LC network shown in the Figure 7 is nothing but the representation of lossless TEM wave propagation on lumped LC element equivalent circuit of a conventional transmission line. So, the phase velocity $V_p = \frac{1}{\sqrt{L'C'}}$ and the characteristic impedance is $Z_c = \sqrt{\frac{L'}{C'}} = \sqrt{\frac{L}{C}}$ which are defined in the case of conventional TL with the assumption that the operating frequency is much less than the cut-off frequency $f << f_c$. Here L’,C’ are per unit length quantities i.e. L’= L/d and C’ = C/d when

'd' is the length of the section of line. Hence from equation (2.31) SWF can be expressed in terms of f_c as

$$\text{SWF} = \frac{\beta}{k_0} = \frac{c_0}{V_p} = c_0\sqrt{L'C'} = \frac{c_0}{d}\sqrt{LC} \tag{2.32}$$

and since $f_c = \frac{1}{\pi\sqrt{LC}}$ we have,

$$\text{SWF} \,.\, f_c \,.\, d = \frac{c_0}{\pi} \tag{2.33}$$

Similarly characteristic impedance Z_c can be expressed in terms of the cut-off frequency f_c as,

$$Z_c \,.\, f_c \,.\, C = \frac{1}{\pi} \tag{2.34}$$

From equations (2.33) and (2.34) we can observe the characteristic impedance Z_c and the SWF are inversely proportional to the cut-off frequency f_c. If we consider Z_c = 50 ohm and for a given operating frequency if the f_c value is set and the unit cell length 'd' is known then by using equations (2.33) and (2.34) one can obtain the SWF and capacitance C values and latter determine the inductance L value.

2.7.2 **Analysis for Characteristic Impedance of Three Circuit lumped element arrangements**

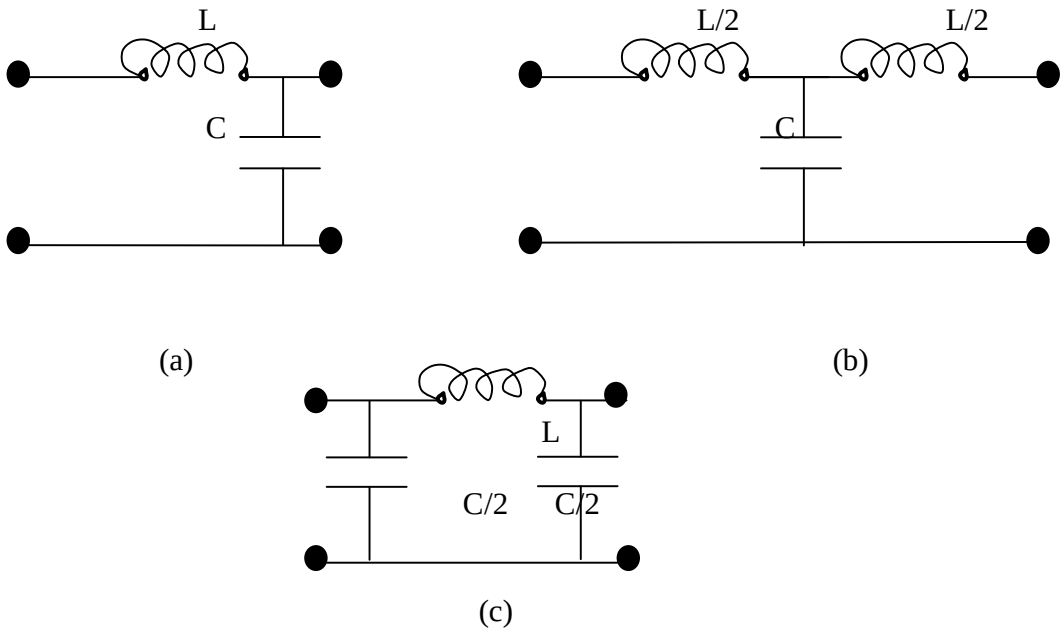

Figure 8 Unit cell in L, T and π form
(a) L-section (b) T-section (c) π – section

There are three combinations possible for low-pass unit cell configuration as shown in Figure.8. The discussions cited till here are only on the assumption that the operating frequency is much less than the cut-off frequency i.e. $f<<f_c$.

To get the complete analysis of the characteristic impedance Z_c we have to study its variation in the above three networks.

The L network is a simple network and the value for the phase constant β is derived from the using this network as shown in equation (2.3). The transmission matrices ABCD for the T and π are different than the L network, but the (A+D) values for same for all the three networks and hence the three networks have the same variations for phase constant. In these symmetrical networks the same is not the case for characteristic impedance Z_c i.e. Bloch impedance as mentioned before. The Z_c value for these three networks can be compared by using the general equation derived in equation (2.27).

First of all considering the case for the 'L' network we have based on the equation (2.27) and ABCD matrix shown in equation (2.28), we can get Z_c as

$$Z_{c_L} \pm = \pm \sqrt{\frac{L}{C}} \sqrt{1 - \frac{\omega^2 LC}{4}} + \frac{j\omega L}{2} \qquad (2.35)$$

Since the above equation for the L network is not symmetrical and also the imaginary part of Z_{c_L} is not equal to '0' this causes $Z_{c_{L+}}$ and $Z_{c_{L-}}$ not equal. If the L network infinite periodic structure is truncated by a load impedance Z_L, then the

reflection co-efficient is expressed as $\rho_L = -\frac{(1-\frac{Z_L}{Z_{cL+}})}{(1-\frac{Z_L}{Z_{cL-}})}$. This makes the value of the characteristic impedance for the L network unstable depending on the number unit cells on the loaded transmission line. We can observe that the Z_c value becomes equal to $\sqrt{\frac{L}{C}}$ which is the same as the conventional transmission line case.

In the second case the ABCD matrix for the symmetrical T network is given

$$\begin{bmatrix} A & B \\ C & D \end{bmatrix}_T = \begin{bmatrix} 1-\frac{\omega^2 LC}{2} & j\omega L(1-\frac{\omega^2 LC}{4}) \\ j\omega C & 1-\frac{\omega^2 LC}{2} \end{bmatrix} \tag{2.36}$$

So, based on equation (2.27) the Z_c of the T network is as

$$Z_{cT} = \sqrt{\frac{L}{C}}\sqrt{1-\frac{\omega^2 LC}{4}} \tag{2.37}$$

In the third case the ABCD matrix for the symmetrical π network is

$$\begin{bmatrix} A & B \\ C & D \end{bmatrix}_{\pi} = \begin{bmatrix} 1 - \frac{\omega^2 LC}{2} & j\omega L \\ j\omega C\left(1 - \frac{\omega^2 LC}{4}\right) & 1 - \frac{\omega^2 LC}{2} \end{bmatrix} \tag{2.38}$$

and

$$Z_{c_\pi} = \frac{\sqrt{\frac{L}{C}}}{\sqrt{1 - \frac{\omega^2 LC}{4}}} \tag{2.39}$$

When we compare the equations (2.35), (2.37) and (2.39) one can observe that the characteristic impedances of the three circuit arrangements can be made equal to $\sqrt{\frac{L}{C}}$ if the operating frequency is very much less than the cut-off frequency i.e. $f << f_c$. The only exception is in the case of L network where there is extra imaginary part. In the case T network Z_c decreases with increase of operating frequency f also Z_c is purely real and where is in the case π network Z_c is directly proportional to the operating frequency f. Both symmetrical networks have the Z_c value changing around the centre value $Z_c = \sqrt{\frac{L}{C}}$ whenever the frequency changes. Thus one determine that the L network is the best choice as it can save more space and if the disadvantages like the imaginary values are negligible then this arrangement is better to design more compact circuit realizations.

The complex propagation constant 'γ' as well as the characteristic impedance Z_c can extracted directly from S-parameter measurements for either of the equivalent circuits. Equations are given as [14],

$$e^{j\gamma L} = \frac{1-S_{11}{}^2+S_{21}{}^2+\sqrt{(1+S_{11}{}^2-S_{21}{}^2)^2-(2S_{11})^2}}{2S_{21}} \qquad (2.40)$$

and

$$Z_c = Z_0 \sqrt{\frac{(1+S_{11})^2-S_{21}{}^2}{(1-S_{11})^2-S_{21}{}^2}} \qquad (2.41)$$

2.7.3 **Dispersion Characteristics**

The quality of the transformer is determined by yet another important factor and it is dispersion. The linear phase response is always desirable in the pass-band to avoid signal distortion for a linear transmission system. The group delay Td can be used as a characteristic for the phase response which is defined as the derivative of the radian phase with respect to the radian frequency [13],

$$T_d = \frac{d\emptyset}{d\omega} \qquad (2.42)$$

Within the pass band a larger value for the group delay corresponds to larger dispersion. It is also referred to as envelope delay, which indicates the delays experienced by the envelopes of transmission packets. Using equation (2.28) for a unit cell 'd', T_d can be expressed as

$$T_d = \frac{d\beta}{d\omega} . d = \frac{\sqrt{LC}}{\sqrt{1-\frac{\omega^2 LC}{4}}} \qquad (2.43)$$

Therefore from the analysis of the transmission line characteristics in the sections from (2.5) to (2.7) one can conclude that in order to obtain reduction in the line size or device miniaturization at a particular frequency one should make the length of the unit cell 'd' as small as possible which corresponds to the SWF being as large as possible according to the equation (2.33). Thus the cut-off frequency f_c can also be lowered but not to reduce too much of the pass-band range. The series inductance as well as the shunt capacitance values also should designed as large as possible within the unit cell.

3. Design of a 1.9 GHz TLT Balun on PCB

Given a unit cell length ‘d’ the question arises as to how should one increase the values for quasi lumped L inductance and C capacitance to the maximum possible also within the smallest unit cell length possible which corresponds to the significant raise in SWF values. The advancement in the current material technology allows the lumped elements to be fabricated practically at a sub-micron level in silicon micro-electronics or at a millimeter-scale on a printed circuit board. Three-dimensional substrate metallization on micro or nano-fabrication of metallic components within di-electrics or semi-conductor substrates has become a key device miniaturization process in the present integrated circuit technology.

3.1 Physical Layout Design

The proposed method is to use a 3-D subsrate metallization approach to develop the quasi lumped elements on the FR-4 standard substrate board. The inductance and the capacitance loadings on a micro-strip line contribute to the quasi-lumped element realization. Both the shunt capacitance as well as series inductance compete for the space on the least unit cell possible for the greatest SWF values. Multilayer 3-D substrate metallization is an efficient solution for the efficient distribution of loading elements into

various layers. The loadings are nothing but fragmented wire, slot, or disc plates that are wound into multiple layers in a periodic manner to make maximally efficient use of the limited 3-D volume.

In this section the TLT or balun realized in Figure 5 is designed using novel ultra slow-wave transmission lines evoloved from the L-network model in order to minimize the line size to the greatest extent possible. Our goal is to design a TLT/Balun that works at the 1.9 GHz frequency.

The proposed Balun is built on 3-layer FR-4 (the relative dielectric constant is €$_r$ = 4.4 and the loss tangent tanφ = 0.02) PCB with the total thickness ‘h’ is 30 mil. The three layer unit cell is shown in Figure 9.

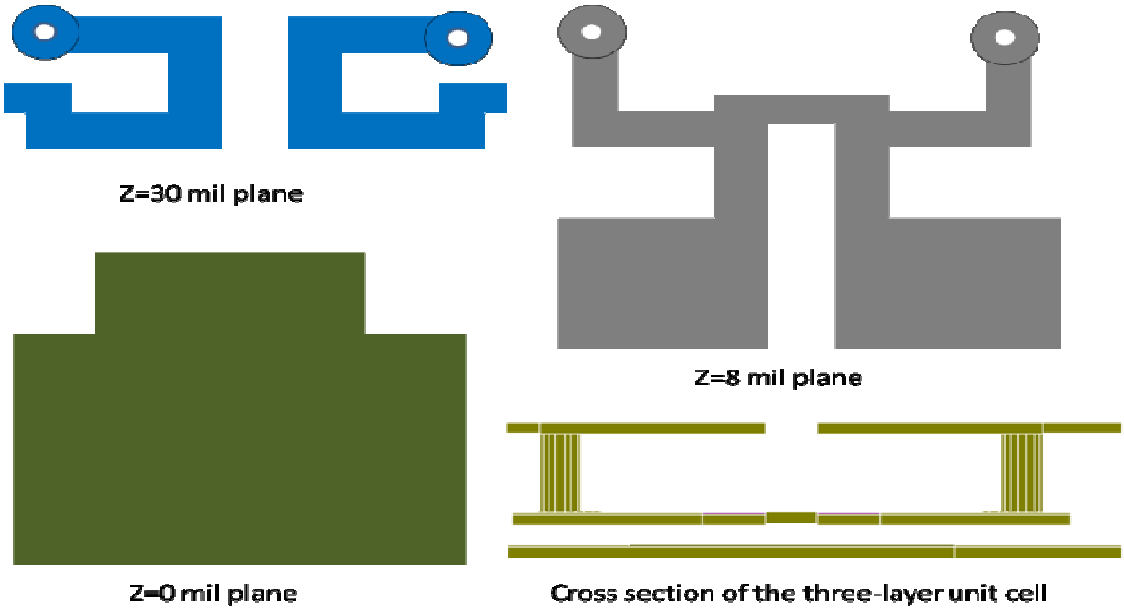

Figure 9 A unit cell of a metamaterial slow-wave transmission line.

To enhance the inductance without using a large die area the use of vertically stacked loops within the multi-layer structure is proposed. In order to obtain a large capacitance in small area, vertically stacked planar inter-digital capacitors can be used on different layers. The number of layers as well as the size of the fingers, distance between them determines the capacitance that can be achieved. These stacked inter-digital capacitors are built over the parallel capacitor to simplify fabrication.

The parallel plate capacitor provides the basis for the total capacitance and its common ground for all the inter-digital capacitors stacked above is its bottom plate.

The vertical stacking is not realized in a simple manner as it is complicated by the vias that must be used for the layer to layer interconnects. Blind-hole vias has a significant cost over through-hole vias, while it further complicates the design. Annular rings are to be attached in both types of vias in order to isolate them and the annular rings have probability of space constraint with the original inductors and capacitors especially when line width and spacing is small.

3.2 **SWF Characteristics**

Two metamaterial slow-wave lines are designed with characteristic impedances equal to 50 ohm and 75 ohm respectively. The simulations of two-port three unit cells are based on IE3D: a method of moment (MOM) based full-wave solver from Zeland. The S-parameters can be used to determine the slow-wave factors as well as the characteristic impedances as derived from the equations (2.40) and (2.41). The simulated slow-wave factors of the 50- ohm and 75 – ohm lines are shown in the Figure 10 shown below.

As seen from the previous derivations the ratio series inductance value to shunt capacitance gives the impedance level and their multiplication gives the slow-wave factor values. 75-ohm line has the larger SWF because of the larger series inductance value L

because of the bigger loops in the Figure 9. Quarter –wave lengths for the two lines at 1.9 GHz based on the SWF vs frequency plot and the previously derived equations are found as 5.7 mm and 4.3 mm for 50 ohm and 75 ohm lines respectively. These two values are used to design the TLT Balun.

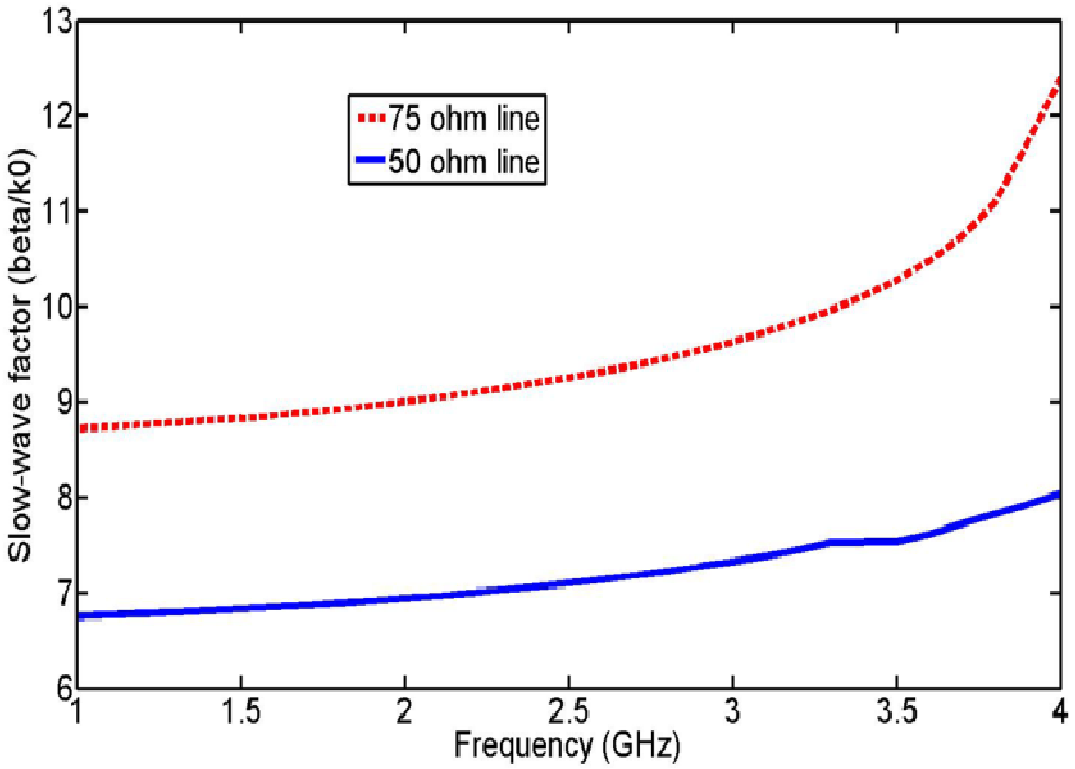

Figure 10 Slow-wave factors of 50 – ohm and 75 – ohm metamaterial transmission lines

3.3 **Design specifications and plots**

A miniaturized TLT/Balun is designed as shown in the Figure 5. It is designed at 1.9 GHz using the novel ultra-slow wave transmission line structures. The isolated inter-connedted TL's on the right side of the Figure 5 are the 75 – ohm lines and the left TL is the 50 – ohm line. According to equation $N = Z_{c2}/Z_{c1}$ where in this case $Z_{c2}= Z_{02}+ Z_{03}$ where in both

$Z_{02}=Z_{03}=75$ ohm and hence $Z_{c2}=150$ ohm,

Now $Z_{c1}= Z_{01}= 50$ ohm,

Hence the N=3. Now the ratio of square of the inverse of the value N determines the impedance ratio and only reciprocal determines the voltage ratio in accordance with the equation (2.20). Therefore we obtained a Balun/TLT with impedance ratio 1:9 and voltage ratio 1:3 at the frequency 1.9GHz. Each line is quarter-wave long at 1.9 GHz. The prototype picture is shown in Figure 11 as shown below.

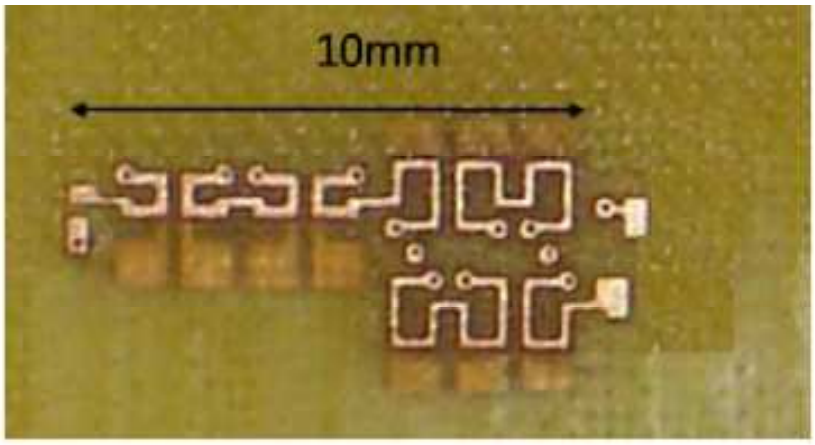

Figure 11 Photograph of a metamaterial TLT Balun prototype

The 50 0hm line has two unit cells with a total length of 5.7 mm and the 75 ohm lines have 1.5 unit cells with a total length of 4.3mm. The total Balun area is 10 mm by 6 mm which is electrically small for a wavelength about 160mm (1.9GHz). Note that two extra vias are necessary to connect 50 ohm and the 75 ohm lines as the two wire lines are opposite side of the di-electric layers.

3.4 **Simulation results and measurement validations**

The simulation results of the TLT/ Balun using Zeland IE3D are shown in Figures 12 and 13 as

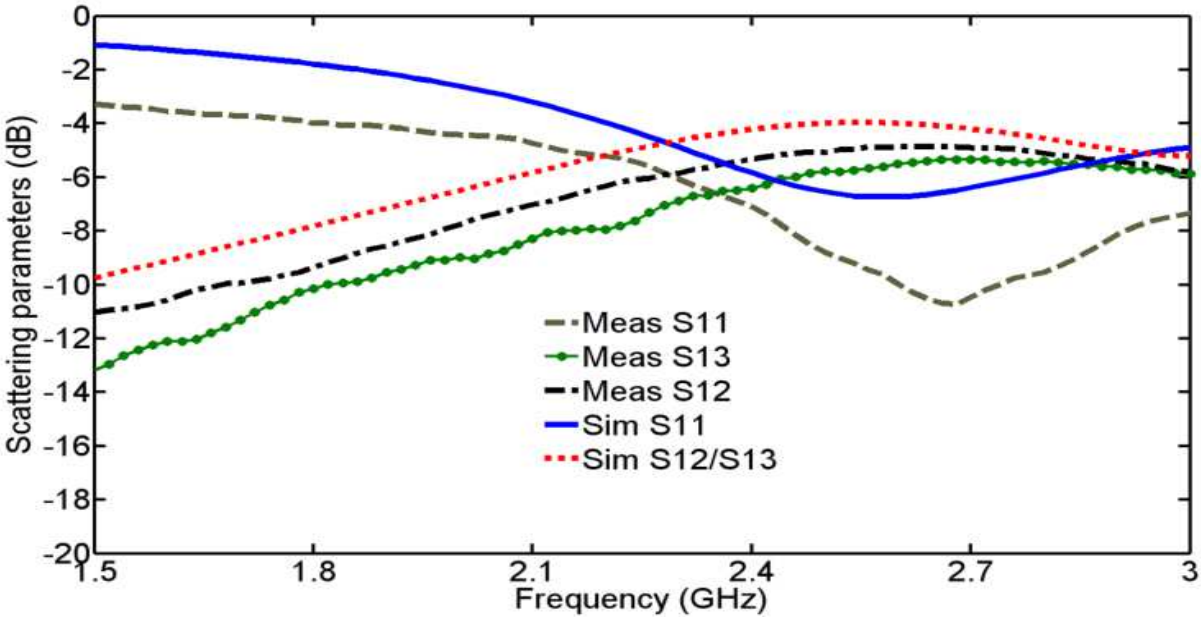

Figure 12 IE3D simulation of the magnitude of S-parameters showing equal power splitting

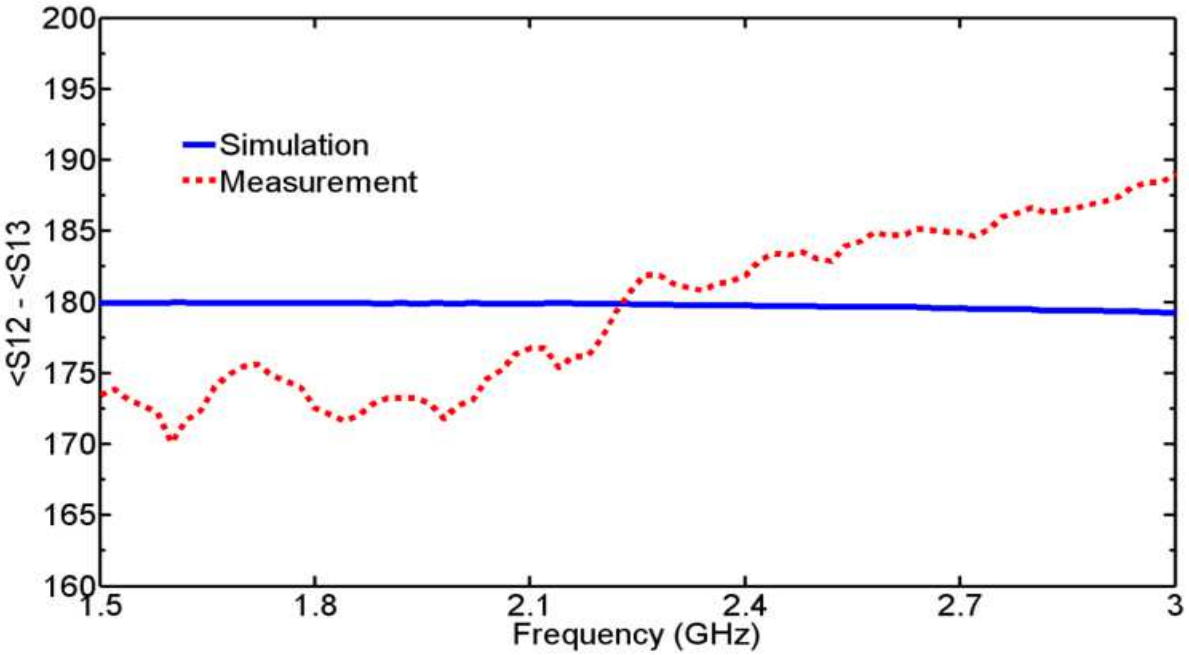

Figure 13 IE3D simulation of the phase difference of the differential output ports

The simulation shows the power splitting between the two output ports and the two output signals are differential (180 degrees) out of phase over a broad frequency range.

The testing of the circuit board shown in Figure 11 presents challenges. SMA connectors are used for measurements. As a result each port requires a transmission line extension and proper de-embedding is needed to extract the S- parameters. A metal is added to the backside of the substrate to act as the ground for the SMA connectors. Figure 14 shows the comparison of the two-port circuit when the output two terminals are treated as one port. The comparison is fair between the measurement and simulation.

For Balun the circuit is 3-terminal device where the input is a single end port and ports 2 and 3 are differential ports. The differential port signals (2 and 3) are identical in magnitude but different in phase by 180 degrees. The three port circuit parameters are measured using a network analyzer where only two-port connection is available. Complete three-port Z-matrix is obtained by performing the two-port measurement three times and in each time one of the ports is open circuited in alternation. The input voltage is normalized to 1 and the output (at the secondary) voltages are the open circuit voltages. In practice either LNA or PA is high impedance and the open circuit voltage is close the actual value.

Frequency response of voltage transformation from primary to secondary from measurements are shown in Figures 15 and 16 as below, for voltage ratio and differential phase respectively.

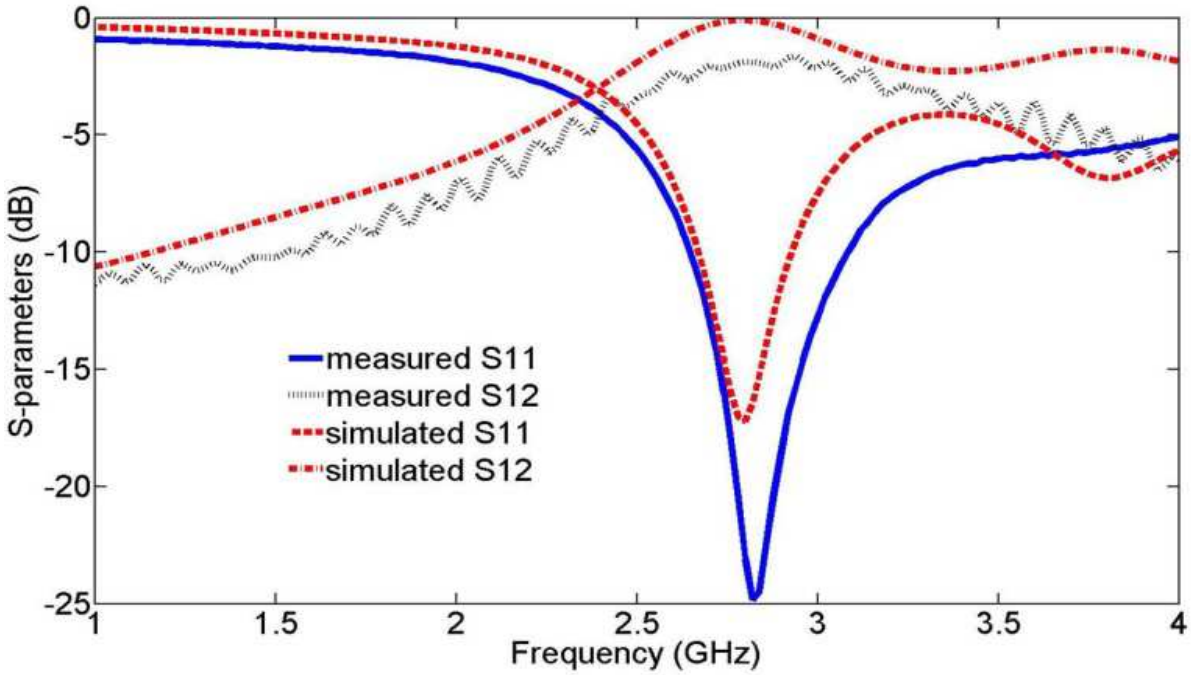

Figure 14 Two-port S-parameter vs frequency when the output differential ports are treated as one port

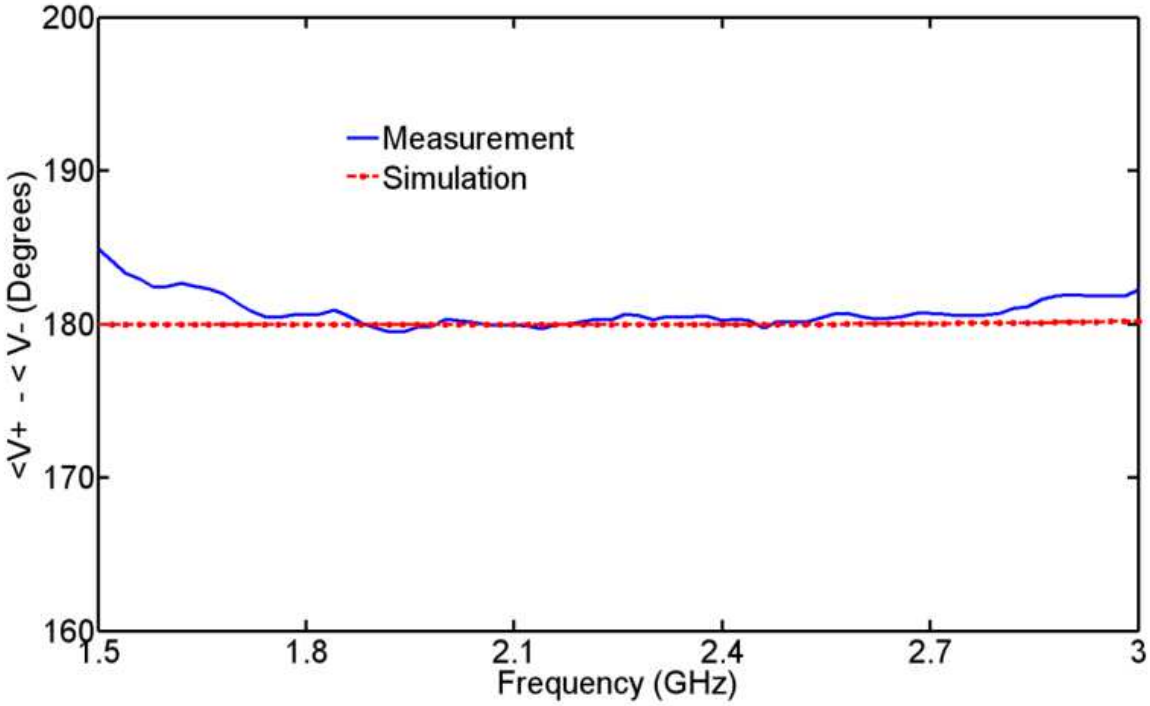

Figure 15 Frequency response of differential phase output at the secondary

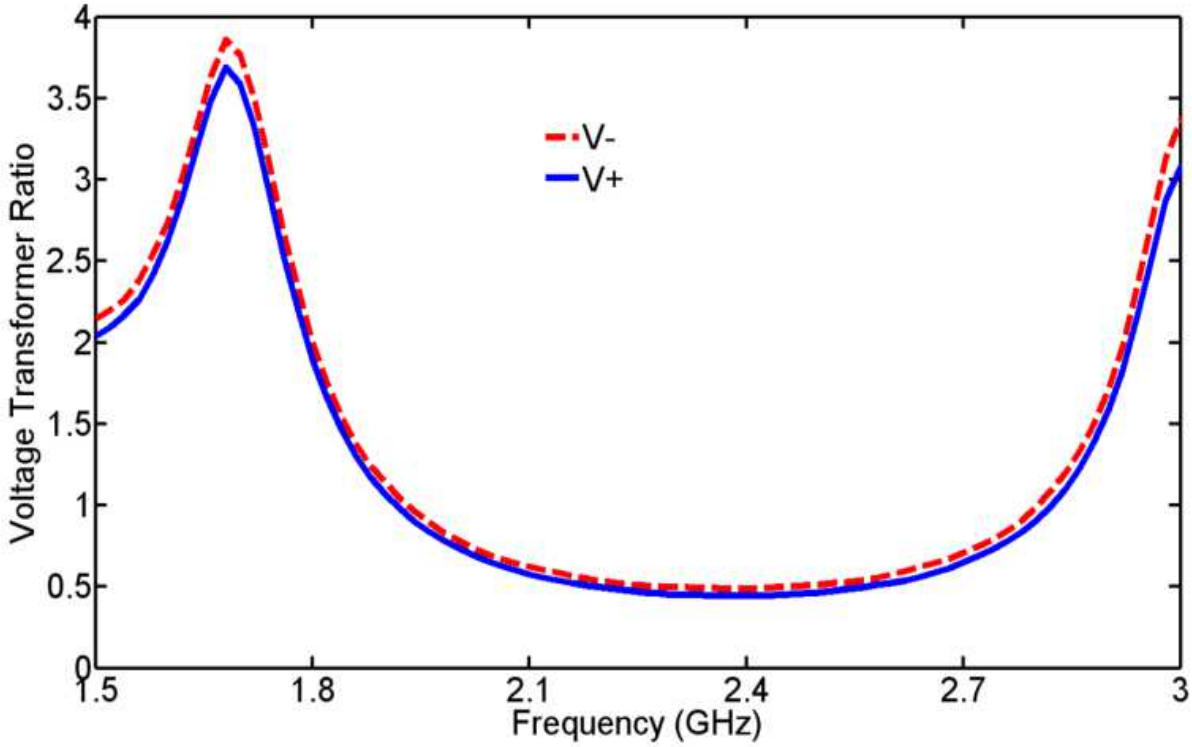

Figure 16 Frequency response of the transformer voltage ratio of the designed on-chip balun

Differential phase response at the output is observed in Figure 16. A better measurement approach which is under pursue is to use on wafer direct 3 port measurement to remove the effect of the SMA and feed line to each port.

Transformer voltage ratio show good balance at the differential output ports upto 1.9 GHz. Note that the design voltage ratio is 1 to 1.5 at 1.9GHz (1 to 3 if it is single end to single end). The measured voltage ratio is around 1.5 at 1.83GHz. The performance is satisfactory.

CONCLUSIONS

This paper presents the hybrid of two break-through novel designs employed to obtain an efficient size reduction in the proposed metamaterial ultra slow-wave transmission line transformer/Balun as well as effective operation at higher frequencies. The first technique is to use a DC isolated planar interconnected transmission lines to obtain the performance as that of a conventional transformer as well electrical isolation for the use of TLT as balun. The second technique is employed to reduce the Balun size to considerable area as low as 10mm by 6 mm which is electrically very small when compared with the guided wavelength 160 mm at 1.9GHz. This technique uses the 3-layer 3-D metallization on a FR-4 substrate of the PCB layout which results in high densities in which loadings are wound into three metal layers (two di-electric layers to increase the slow-wave factor dramatically. In contrast to the Marchand Baluns the proposed Balun is DC short in the primary and DC isolated in the primary and secondary. The two differential output-ports are next to each other but at different layers.

A balun prototype was designed, fabricated and tested for 1.9 GHz. Two quarter-wave metamaterial inter-connected lines of 50 ohm and 75 ohm characteristic impedances each interconnected with vias are used to for the Balun. The test results show good Balun performance.

This thesis showed one of the many design approaches towards designing highly dense and compact fabrication of the RF components in the SOC and RFIC realizations. Ultimate goal is to however design many other RF components using multilayer substrate technology with greater and novel size reduction techniques and also for efficient operation at much higher frequencies.

REFERENCES

[1] C. L. Rutherford, "Some broad-band transformers," Proceedings IRE, vol 47, pp. 1337 -1342, 1959.

[2] M. A. Morrill, V. A. Caliskan, and C. Q. Lee, "High frequency planar power transformers," IEEE Trans. On Power Electronics, vol 7, no. 3, pp. 607-613, July 1992.

[3] A. Lai, T. Itoh, C. Caloz, "Composite right/left-handed transmission line metamaterials," *IEEE Microwave Magazine*, , vol. 5, no. 3, pp. 34 – 50, September 2004.

[4] C. Zhou and H.Y.D. Yang, "Design Considerations of Miniaturized Least-Dispersive Periodic Slow-Wave Structures," *IEEE Trans. on Microwave Theory and Techniques*, vol. 56, no. 2, pp. 467-474, February 2008.

[5] J.J. Zhou and D.J. Allstot, Monolithic transformers and their application in a differential CMOS RF low-noise amplifer," *IEEE Journal of Solid-State Circuits*, vol. 33, no. 12, pp. 2020-2027, Dec. 1998.

[6] W. Simburger, H. Wohlmuth, P. Weger, and A. Heinz, "A monolithic transformer coupled 5-W silicon power amplifier with 59% PAE at 0.9 GHz," *IEEE Journal of Solid-State Circuits*, vol. 34, no. 12, pp. 1881-1892, Dec. 1999.

[7] John R. Long, "Monolithic transformers for silicon RFIC design," *IEEE Journal of Solid-State Circuits*, vol. 35, no. 9, pp. 1368-1382, Sep. 2000.

[8] H.Y.D.Yang and J.A. Castaneda, "Design and analysis of on chip symmetric parallel-plate coupled-line balun for silicon RF integrated circuits," 2003 *RFIC Symposium*, pp. 527-530, Philadelphia, June 13, 2003.

[9] Pervez. A. Dalal, "High Frequency Coreless Transmission Line Power Transformers", MS Thesis, University of Illinois at Chicago, Chicago, 1995.

REFERENCES (Continued)

[10] C. W. Davidson, Transmission Lines for Communications. MacMillan Education Ltd., Hong Kong, 2nd Ed., 1989, pp.74.

[11] G. L. Matthai, L. Young, and E. M. T. Jones, "Microwave filters Impedance Matching Networks and Coupling Structures", McGraw Hill, N.Y., 1964.

[12] C. W. Allen and H. L. Krauss,"Wide-Band Rotary Transformer-Unbalanced Current Analysis," IEEE trans. MTT, pp. 200-205, May 1976.

[13] D. M. Pozar, *Microwave Engineering*., New York: Wiley, pp. 66, 1998.

[14] W. R. Eisenstadt, and Y. Eo, "S-Parameter based IC Interconnect Transmission Line Characterization," *IEEE Trans. Components, Hybrids, and Manufacturing Tech*., vol. 15, pp. 483-490, Aug. 1992.

BIBLIOGRAPHY

[1] C. W. Davidson, Transmission Lines for Communications. MacMillan Education Ltd., Hong Kong, 2nd Ed, 1989.

[2] G. L. Matthai, L. Young, and E. M. T. Jones, Microwave filters.Impedance Matching Networks and Coupling Structures. McGraw Hill, N.Y., 1964.

[3] K. C. Gupta R. Garg, and I. J. Bahl, Microstrip Lines and Slot lines, Artech House, 1979.

[4] R. E. Collin, Field Theory of Guided Waves, IEEE press, NY, 2nd Ed, 1991.

[5] T. Itoh, Planar Transmission Line Structures, IEEE press, 1987.

[6] Robert S. Elliot, An Introduction To Guided Waves and Microwave Circuits, Printice Hall, Inc. , 1993.

[7] D. M. Pozar, *Microwave Engineering*., New York: Wiley, 1998.

VITA

NAME:	Vamsee Krishna Chekka
BIRTHPLACE:	Vijayawada, INDIA.
EMAIL:	vamsee.ch5@gmail.com
EDUCATION:	B.Tech., Electronics and Communications Engineering, Acharya Nagarjuna University, A.P., INDIA, 2008. M.S., Electrical and Computer Engineering, University of Illinois at Chicago, Chicago, IL, 2012.
PROFESSIONAL MEMBERSHIPS:	IEEE Antennas and Propagation Society, Student member. IEEE Microwave Theory and Techniques Society, Student member.
PUBLICATIONS:	H.Y.David Yang, Vamsee K.Chekka and Haijiang Ma,"*Slow-Wave Transmission Line Transformers/Baluns*", Digest of IEEE International Microwave Symposium, Anaheim, CA, May 23-28,2010.
SKILL SET:	Technical: ANSOFT HFSS, IE3D, Verilog HDL, MATLAB, ADS, Simulink, PSpice Computer Languages: C, C++, ASP.NET and Data Structures Web Design/Graphic Tools: HTML, Dream Weaver, Macromedia Flash, Adobe Photoshop Test Equipments: Spectrum Analyzers, Network Analyzers, Hybrid Couplers, Power Dividers, Signal Generators, RF Multiplexers and Power Meters.